6-8-2022

Infrared Thermal Images of Solar PV Panels for Fault Identification Using Image Processing Technique

Victor Kirubakaran

D. M. D Preethi

U. Arunachalam

Yarrapragada K. S. S Rao

Mansour K. Gatasheh

See next page for additional authors

Authors

Victor Kirubakaran, D. M. D Preethi, U. Arunachalam, Yarrapragada K. S. S Rao, Mansour K. Gatasheh, Nasrul Hoda, and Endalkachew Mergia Anbese

Hindawi

Research Article

Infrared Thermal Images of Solar PV Panels for Fault Identification Using Image Processing Technique

V. Kirubakaran [1], **D. M. D. Preethi,**[2] **U. Arunachalam,**[3] **Yarrapragada K. S. S. Rao,**[4] **Mansour K. Gatasheh,**[5] **Nasrul Hoda,**[6] **and Endalkachew Mergia Anbese** [7]

[1]*Centre for Rural Energy, The Gandhigram Rural Institute, Gandhigram, Dindigul, Tamilnadu, India*
[2]*Department of Computer Science and Engineering, PSNA College of Engineering and Technology, Dindigul, Tamilnadu, India*
[3]*Department of Mechanical Engineering, University College of Engineering-Nagercoil, Tamilnadu, Nagercoil, India*
[4]*Department of Mechanical Engineering, Aditya College of Engineering, Surampalem, 533437 Andhra Pradesh, India*
[5]*Department of Biochemistry, College of Science, King Saud University, P.O. Box 2455, Riyadh 11451, Saudi Arabia*
[6]*Department of Neurology, Henry Ford Health System, Detroit MI 48292, USA*
[7]*Department of Civil Engineering, Ambo University, Ambo, Ethiopia*

Correspondence should be addressed to Endalkachew Mergia Anbese; endalkachew.mergia@ambou.edu.et

Among the renewable forms of energy, solar energy is a convincing, clean energy and acceptable worldwide. Solar PV plants, both ground mounting and the rooftop, are mushrooming thought the world. One of the significant challenges is the fault identification of the solar PV module, since a vast power plant condition monitoring of individual panels is cumbersome. This paper attempts to identify the panel using a thermal imaging system and processes the thermal images using the image processing technique. An ordinary and thermal image has been processed in the image processing tool and proved that thermal images record the hot spots. Similarly, the new and aged solar photovoltaic panels were compared in the image processing technique since any fault in the panel has been recorded as hot spots. The image recorded in the aged panels records hot spots, and performance has been analyzed using conventional metrics. The experimental results have also been verified.

1. Introduction

The usage of renewable energy is increasing daily to give a sustainable and clean form of energy. The recent day's use of solar energy has grown tremendously. Both rooftop and ground-mounted technologies penetrated the market at a rapid phase. In the same way, the operation and maintenance of solar panels also need to be taken care of. Solar PV systems are maintenance-free; however, the system's monitoring is essential to achieve the maximum yield from the plants. Several parameters affect the panel output like dust, humidity, shadow temperature, and moisture. In an extensive power plant, monitoring of individual panels is a cumbersome process. However, any parameters affecting the yield of solar panels will induce internal resistance. Thus, a thermal image of the panels will be able to identify the fault of the panel quickly. Several thermal imagers are readily available in the market; analyzing individual images is a difficult task. Hence, the picture taken in a thermal imager is processed by MATLAB Simulink software for the different steps in the images' layering. The temperature difference is associated with bordering the modules, and hot spots are easily identified.

2. Literature Review

Different types of solution for the fault detection and the analysis by the various steps such as monitoring systems, I and C analysis based on artificial intelligence, and voltage and current measurements and also by power loss measurements analysis process of the different methods have no

precise data and not decentralized in the system for inverters and to fault diagnosis [1–3]. Electrical degradation of old panel and its working defects via IR thermography and VI characteristics and also the simulation in MATLAB and from this study of image processing of the PV panel with the software by an algorithm were discussed [3, 4]. Evaluation of the solar PV system to grid connections and the solar PV system simulation with the MATLAB software the assessment of the full operating power plants were conducted [4, 5]. Comparison between the regular model and expected values of the proposed system by the different types of shading and their output readings for the fault system on PV was performed, and the noise for detection time for these outputs and graph is drawn, and stability curve is also made for respected data [5, 6]. To compare in faulty condition threshold with system operation in nominal condition, there are many approaches and the choice of one technique depends on the following: knowledge of the history of system events, the expert system knowledge, data collected on the system in normal operation conditions, a known model of the system, fault types of the short circuit, open circuit, mismatch of loads, and ground faults by the serious of coding by the data acquired by the control system in the system via MATLAB to indicate which type of defect has occurred on the system [6, 7]. Infrared imager for solar panels provides the data and converts it to the CIELAB (it is 3D color space that enables accurate measurement and comparison of all perceivable colors using three color values), and segmentation by processing the panel of different cells, modules, and dust forming increases the temperature of different sizes and temperature ranges [8, 9]. The relationship between the different panels' dust density and spectral transmittance is determined. The slope angle outcome is rightly linked to the quantity of dirt thickness difference on the outward. Dirt adds to the decrease of PV production by decreasing irradiance in a spectrally reliant manner [10, 11]. This is viewed as the result of the spectral answer data. The outcome is not a similar amount for all sorts of PV technology for spectral conduction that disturbs numerous spectral reply forms [12, 13]. Solar modules are to be viewed as the single cells for the identification of each by the industrial control computer. Then, for the different sets of the problems like the broken grid, fragmented cells, black pieces on solar cells, and cracks on the cells, the different sets of methods are used to identify the fault and analyses with which level of the defects are in it. It provides very accurate and high real processing time [14, 15]. Thermal image processing of the solar PV modules is used. It represents the various steps for the modules' changes for the identification of the fault [16, 17]. They mainly assumed on the three different faults as the heavy, minor, and medium faults. However, this paper deals with thermal imaging technique to detect exact fault in the cells The characteristic curves have been plotted to find out the difference in the spots and healthy ones. This model comprises the electrical and mechanical systems and then provides an optimal solution for the systems' MPPT conditions [18, 19]. Identification of the fault in the solar PV modules is done by the cutting edge technology and by the nondestructive testing methods like the thermal image process. In this paper, a neural network classifier-based algorithm is developed with the different sets of conditions and the collections of the modules to attain the perfectness for the deduction of the fault [20, 21]. After the test algorithm is created, it is verified by the thermal image, which is then converted to the gray image, and then, it is subjected to linear filtering [22]. The intensity gradient is adjusted and then for the hysteresis thresholding, the values at last were identified with the cutting edge technology. The image is then Hough transformed to the binary image, and the Hough lines are peaks on them to identify the faults and the efficiency of the increased than other methods. Solar PV module faults in the only way to show the necessity of the fault detection in the solar modules [23]. The solar modules got fired at California and North Carolina which are showed as the examples of the faults. The EL images are taken for the healthy panels and the spots of the minor cracks, break images, and finger impregnations for fault-finding. Then, by the PCA and ICA for the image to be processed by the component analysis. The differentiation from the healthy panels and finding the exact defects in them for the MATLAB software to find without the exact defects save the faults' cost and reliability [24].

3. Solar PV Panel

3.1. Solar Photovoltaic Cell. The solar PV cell comprises the solar panel. They are made of silicon-based semiconductors and photons of light that transfer electrons to energy when sunlight passes on a PV cell; the PV cell may be reflected and absorbed or pass right through it, converting the light energy into the electrical power. The solar cells are used to make the solar array, which comprises the solar module to generate electricity. This process was explained in the above solar cell figure. The solar cells work high on maximum insolation, making the device work under high-efficient conditions. The solar array is made of solar panels in series and parallel combinations to get the designed voltage and current level. Figure 1 represents a single solar cell.

3.2. Solar Energy Conversion Principles. There are two modes of tapping energy from the sun. The first one is the solar thermal method, and the second one is the solar photovoltaic method. PV modules and arrays are just one part of a PV system. This system includes installing solar panels that convert direct current (DC) to Alternative Current (AC) electricity for appliances in your home. The solar photovoltaic method is used in the experiment; the solar photovoltaic panel is based on the conversion principle that when light falls on the semiconductor, the energy is released and makes electrons flow in the form of the electrical power; this is the primary conversion of the PV system. Figure 2 shows the solar PV panel.

3.3. Thermal Imager. A thermal imaging technique is an image capturing method that converts the original appearance of an object with the heatwave and stores in a digital format without any contact of the item. Figure 3 shows the thermal imaging camera, which will capture any object and give the thermal color coding using infrared techniques. FLIR maker thermal imager is represented in Figure 3.
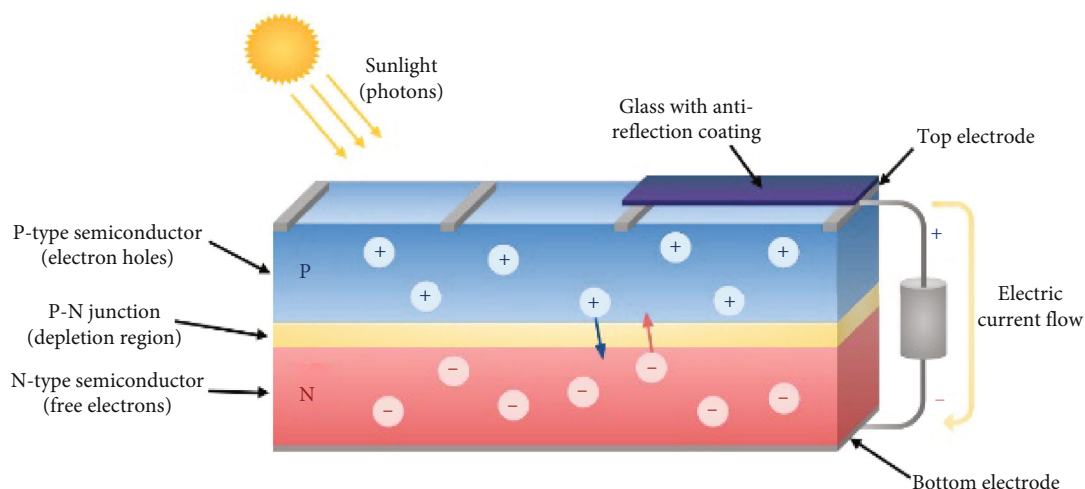
FIGURE 1: Solar cell.

FIGURE 2: Solar panels.

FIGURE 3: Thermal imager.

4. Proposed System

The planned system is aimed at finding out of fault to have occurred in solar photovoltaics in the initial stages. The FLIR's thermal images can do this about the solar PV panels. The thermal images taken are to be processed by MATLAB by the coding. This can be provided with the flow chart process in Figure 4.

5. Methodology

The system comprises the renewable energy source and the fault to be detected by the different images' different sources

to change in the product to be carried out by the image processing. The flow chart provides the necessary data and how the things are to be done by the system with the help of MATLAB. As the software plays a significant role in the project which is to make the images be processed by it to provide the difference of the pictures which we were given as the input to make the effective output way to analyze them with the original images so that the fault is found out easily which is shown in Figure 4. At first, in fault-finding, the images provide the absolute image processing of the solar panels. So the experiment is to carry out on a metal plate that is heated in a particular place [25]. It is then taken as the thermal image, grayscale image, and familiar color image by the thermal imager. It is processed under the software, whereas the thermal spikes are getting known to show accurate data. After experimenting with the metal plate, the old panel is subjected to the result's undergoing process to find out the faulty one.

5.1. Preprocessing Unit. Initially, a novel image is converted to a grayscale image. And then, it undergoes the image processing algorithm, which is to differentiate the images.

5.2. Intensity Adjusted Image. It has changed the intensity adjusted of the novel image to get an accurate image in them.

5.3. Morphological Dilated Image. The image then identifies the morphological data to which the unnecessary parts have been removed concerning the original image on the input given for processing the image.

5.4. Cell Structure Removed Image. Then, the image identified the morphological data to which the unnecessary parts have been released concerning the original image on the input given for the processing of the image and the cell structure removing in this stage of the process.

5.5. Mask for Solar Panel. The initial stage is to remove the sections that stake the defects in their features like the hot spot. The subsequent step is to recognize hot spots and cell structure. A hot spot that comes into view in the image can be traced using the Hough transform (HT). The Hough transform is a
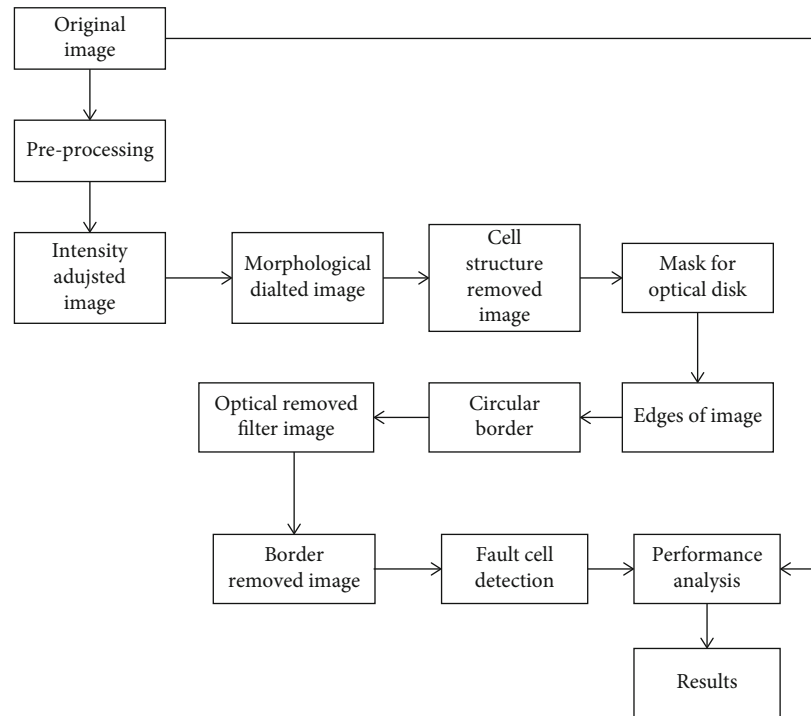
FIGURE 4: Flow diagram of the proposed system.

technique which can be used to isolate features of a particular shape within an image. Because it requires that the desired features are specified in some parametric form, the classical Hough transform is most commonly used for the detection of regular curves such as lines, circles, and ellipses. The results obtained in the HT are presented in Figure 4.

5.6. Edges of the Image. To make a clear image on the plate system, images are taken to identify the edges of the images sent to the process, the data for the identification. To plot the outer parts, it shows with the structure.

5.7. Circular Border of the Image. The circular border of the image is the different sets of options to provide the circular structure of the data. It is used to identify the edges of the pictures and the spikes from the pixel's variations' input image indifference.

5.8. Hot Spot Identification Image. It provides the hot spots the filtered image on that to make the difference the edges removed, and the visually seen the picture of the input, then it allowed for the processing.

5.9. Border Removed Image. After the hot spots from the circular border image are identified, the border region is removed to get a clear image of the fault's cell structure in the processing data.

5.10. Fault Cell Detection. The Hough transform can identify the fault located on the cell. It is used to remove the border region. The initial point for the transformation is referred to as a marker.

The morphological reconstruction algorithm is to get the final estimate of the hot spot. The MATLAB operations are listed in Table 1.

6. Experimentation and Results

For the experimentation process, the three different images are being taken. In that one is a thermal image of the metal plate, and the other is the grayscale image of the metal plate, and the last one is the color image of the metal plate. These images are being processed on MATLAB with the coding. The experimentation results for the thermal image with the hot spot of metal plate processed with the software are given in Figure 5.

The experimentation results for the metal plate's gray image with hot sport processed with the software are given in Figure 6.

The experimentation results for the normal image with the hot sport of the metal plate processed with the software are shown in Figure 7.

The hot spot is viewed in the thermal image from the above three different sets of image processing data. It is obvious that image processing of thermal images exactly identifies the hot spots. Most of the parameters affecting the solar panels induce internal resistance and give the hot spots which cannot be easily identified. However, the thermal images will detect hot spots. If image processing tools can be employed, the exact hot spots will be easily located.

To ascertain the same, a comparison between aged and new panel thermal images has been analyzed using image processing techniques. It is represented in Figures 8 and 9.

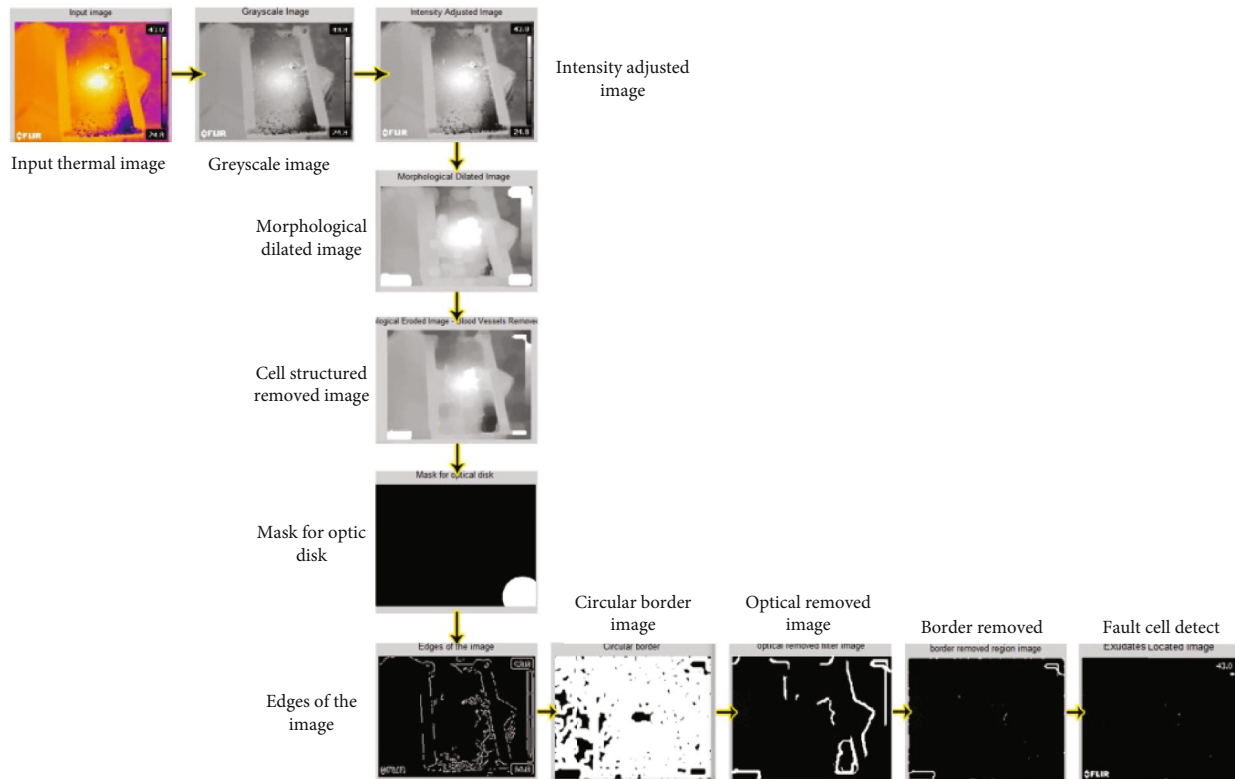| MAT LAB functions and their explanations	
Imadjust (I)	Gray image intensity values
Imdilate (IM, SE)	Dilates the grayscale
Imerode (IM, SE)	Sonnet the grayscale
Median (A)	Vectors have assigned for the column "A"
Floor (A)	Converts the number to the nearest integer
Meshgrid (abc, def)	Duplicates the abc and def to arrive final grid
Edge (I, "canny," thresh)	Low and high value considered as a first and second element to get the threshing
Logical (A)	Produces final value from numerical
Adapthisteq (I)	Improve the image

FIGURE 5: Thermal image processed.

7. Validation

Thermal image of the solar panel quality has been accessed using conventional parameters. New panel thermal image and the aged panel thermal image have been captured using thermal imager with size 300×345 pixels with a resolution of 96 dpi. ANOVA built in MATLAB is used for error analysis.

7.1. Conventional Parameters. Due to aging, the solar cells degraded which increased internal resistance. This may be recorded as hot spots in the thermal images of the solar panel. Hence, the new panel thermal image has been taken as bench mark image. Based on the bench mark image, the quality of the other panel thermal images has been verified using correlation quality (CQ), correlation coefficient (CC), normalized cross-correlation (NCC), image fidelity (IF), normalized mean square error (NM), signal-to-noise ratio (SNR), peak signal-to-noise ratio (PSNR), and mean square error (MSE). Correlation quality (CQ) is a measure of probability indices of measured and calculated quality of images which can be calculated using the following equation:

$$CQ = \frac{\sum_{p,q} I_{p,q} \sim I_{p,q}}{\sum_{p,q} I_{p,q}}. \tag{1}$$

Correlation coefficient has been obtained from the following equation:

$$CC = \frac{\sum_{p=1}^{q} I_{p,q} * \sim I_{p,q}}{\sqrt{I_{p,q}^2} * \sqrt{\sim I_{p,q}^2}}. \tag{2}$$
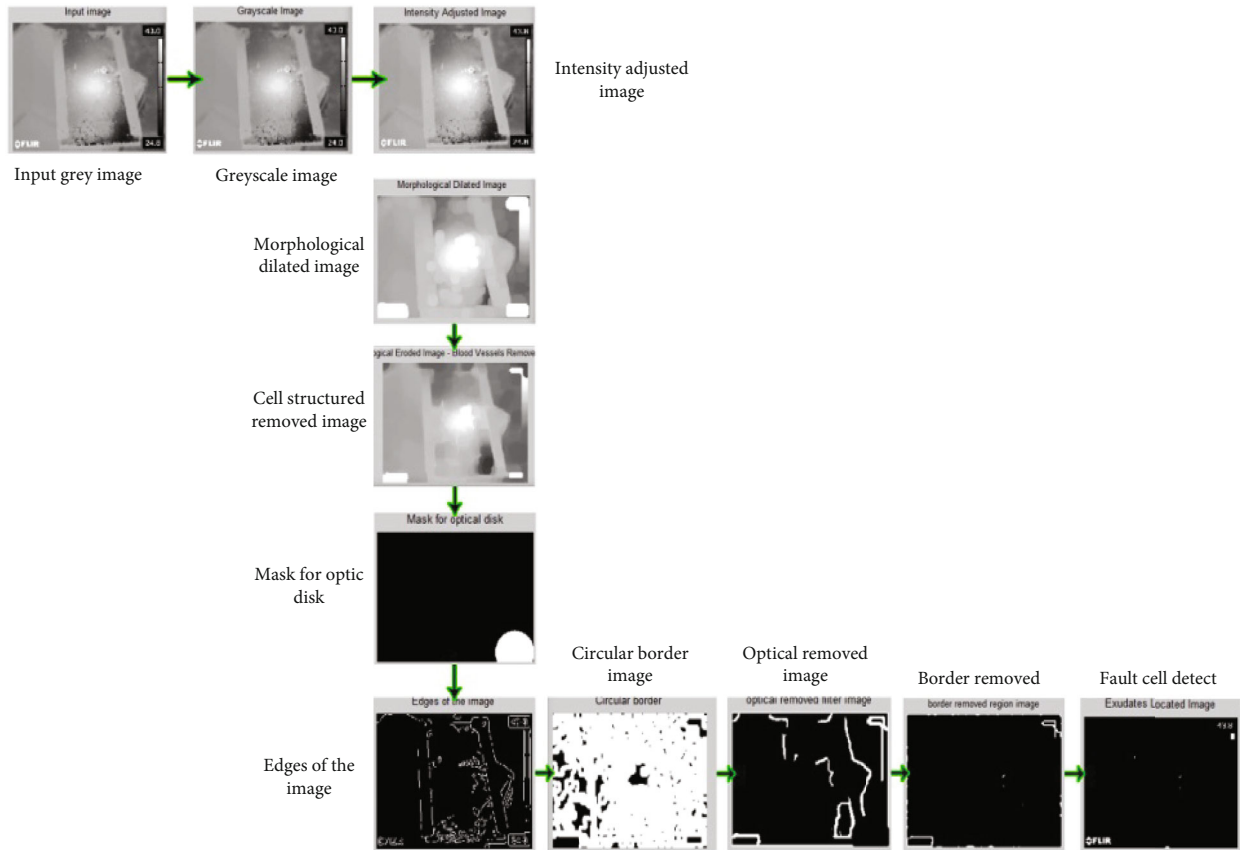
FIGURE 6: Metal plate's gray image with hot sport processed.
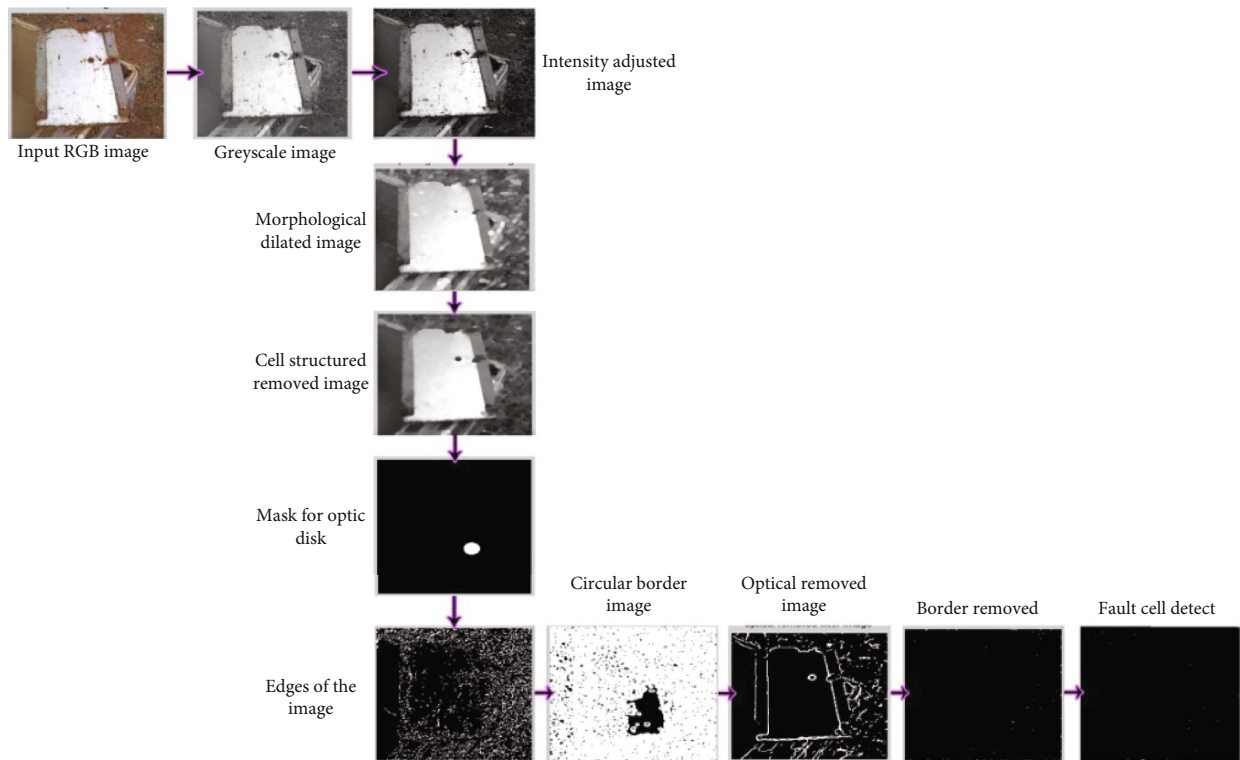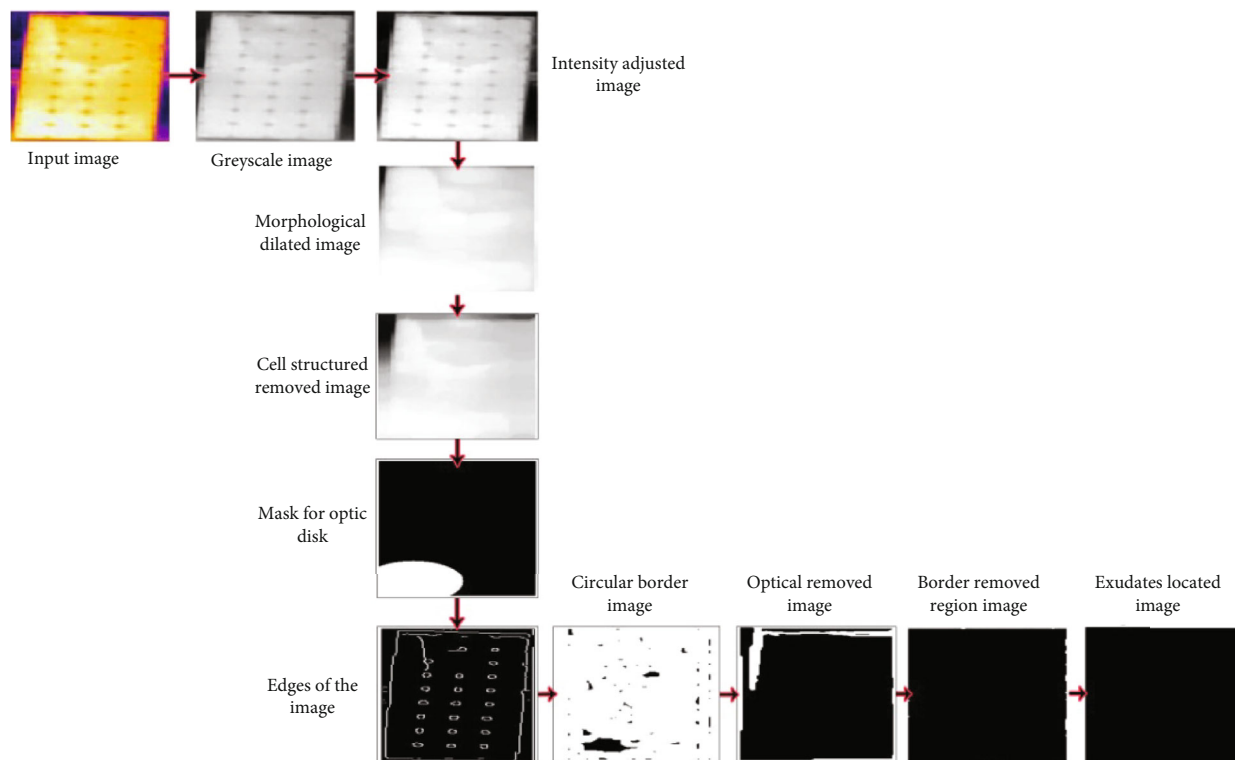

FIGURE 7: RGB image processed.
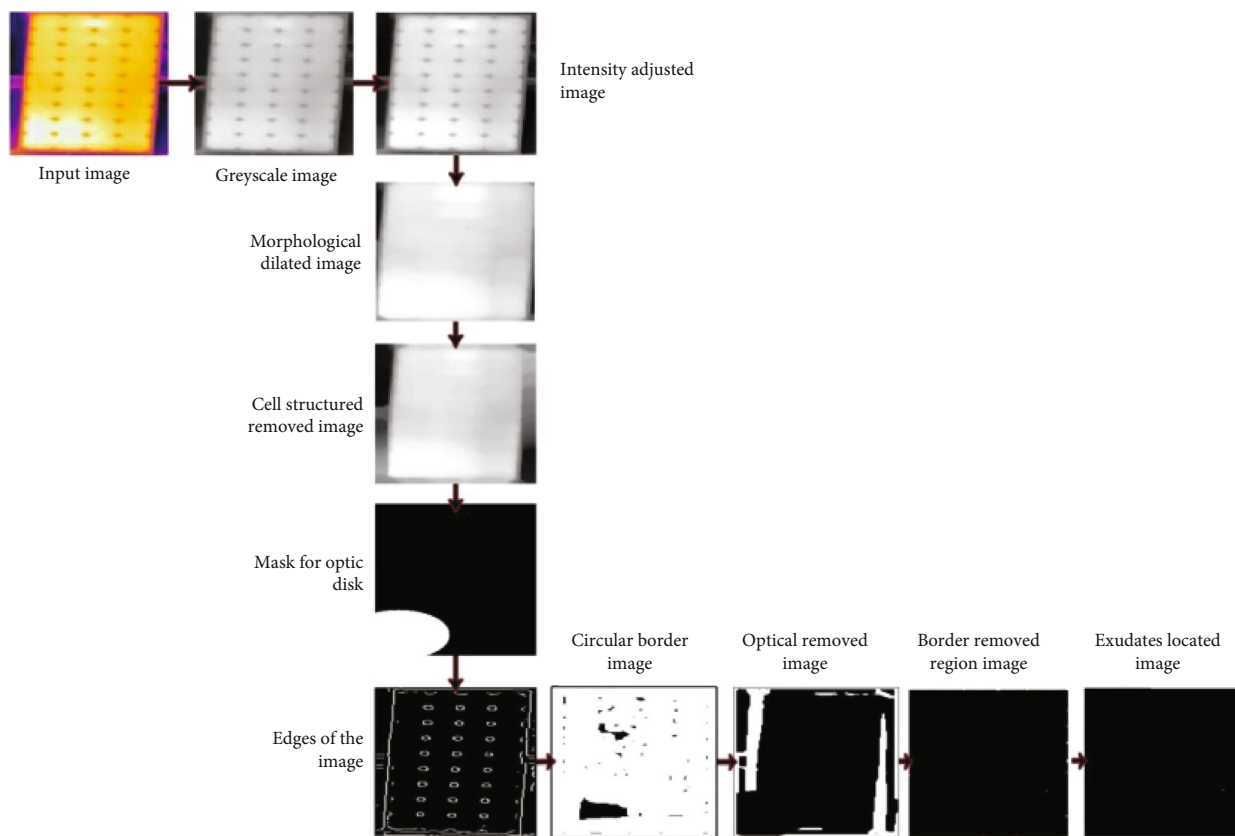
Figure 8: Aged solar panel thermal image processed.

Figure 9: New solar panel thermal image processed.

TABLE 2: Conventional metric indices.

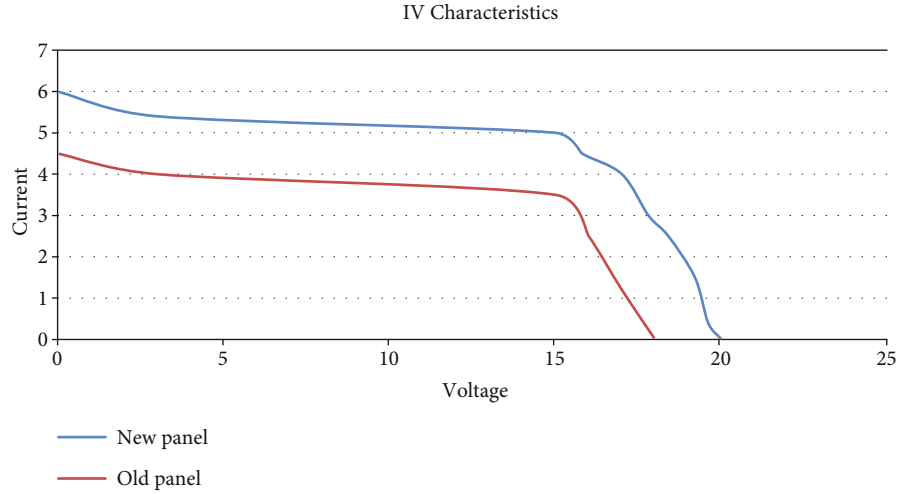| Thermal image	CQ	CC	NCC	IF	PSNR	SNR	MSE	NMSE
TD1	$7.9818e^{+11}$	0.9993	$1.8305e^{+14}$	$-8.7549e^{+09}$	+20.02db	$8.7549e^{+09}$	0.0100	$4.8645e^{-05}$
TD2	$9.3287e^{+11}$	0.9627	$1.4325e^{+14}$	$-6.1287e^{+09}$	+17.52db	$5.2375e^{+09}$	0.0098	$5.2972e^{-05}$
TD3	$6.2879e^{+11}$	0.9843	$2.8792e^{+14}$	$-4.2789e^{+09}$	+15.42db	$1.5287e^{+09}$	0.0201	$3.2147e^{-05}$
TD4	$9.2234e^{+11}$	0.9332	$2.0078e^{+14}$	$-9.1879e^{+09}$	+27.22db	$3.2489e^{+09}$	0.0096	$5.2278e^{-05}$
TD5	$5.8978e^{+11}$	0.9775	$1.9278e^{+14}$	$-6.1978e^{+09}$	+15.22db	$2.8792e^{+09}$	0.0899	$5.9278e^{-05}$
Quality	Poor	Good	Poor	Poor	Poor	Poor	Poor	Poor

FIGURE 10: IV characterization of TD1 and bench mark solar panel.

Normalized crosscoordinate (NCC) is identical to the value of CC and computed using the following equation:

$$NCC = \frac{\sum_{p,q} I_{p,q} \sim I_{p,q}}{\sum_{p,q} I_{p,q}^2} \qquad (3)$$

Image fidelity is used to compute the changes in the images which is calculated using the following equation:

$$IF = 1 - \frac{\sum_{p,q} \left(I_{p,q} - \sim I_{p,q}\right)^2}{\sum_{p,q} I_{p,q}^2}. \qquad (4)$$

PSNR indicates peak signal-to-noise ratio of bench mark image which is computed using the following equation:

$$PSNR = \frac{M \sum_{p,q} I_{p,q}^2 N}{\sum_{p,q} I_{p,q} - \sim I_{p,q}^2}. \qquad (5)$$

SNR estimates the quality of the degraded images and is represented by the following equation:

$$SNR = \frac{\sum_{p,q} I_{p,q}^2}{\sum_{p,q} I_{p,q} - \sim I_{p,q}^2}. \qquad (6)$$

MSE is used to measure the degradation of image and computed by the following equation:

$$MSE = \frac{1}{MN} \sum_{p,q} \left(I_{p,q} - \sim I_{p,q}\right)^2. \qquad (7)$$

NMSE represents high degradation and is computed using the following equation:

$$NMSE = \frac{1/MN \sum_{p,q} \left(I_{p,q} - \sim I_{p,q}\right)^2}{\sum_{p,q} \left(I_{p,q}\right)^2}. \qquad (8)$$

The CQ and NC must be high, and IF, MSE, NMSE, and SNR must be low for the threshold value for the quality comparison. 20 and 40 db is ideal for PSNR values, and CC should be between 0.8 and 0.98. One-way ANOVA which is inbuilt in MATLAB has been performed for validating the conventional indices. Conventional metric indices are reported in Table 2.

From the above values, it has been inferred that the degraded panels' thermal image quality has been reduced compared with the new panel thermal image. Hence, the proposed thermal imaging technique is an ideal tool for fault identification and quality of the solar cell can be easily monitored, along with the conventional IV characteristics of the aged (TD1) and new panel (bench mark) of 75-watts capacity, which

is carried out and reported in Figure 10. The efficiency of the new panel (bench mark) is about 11.62%, and the efficiency of the aged (TD1) panel is about 6.32%, and the Voc and Isc of the new panels are about 22 V and 6.06 A, and for the aged panels are about 20 V and 5.8 A, respectively, and it is shown in Figure 10. By conventional methods, IV curve is traced.

8. Conclusion

Condition monitoring of large solar power plants is the need of the hour. Analyzing the individual string or panels is a difficult task. Most of the fault in the solar panels are recorded as hot spots due to increased internal resistance. Difference image processing techniques with the different coding in MATLAB have been incorporated to identify the hot spots. From the resultant sets of images of the metal plate with hot sports, it is evident that the thermal image can quickly locate hot spots using the Hough transform technique. The same coding has been tested for aged and new panels, and the hot spots have been recorded in the aged panels since the internal resistance of the aged panels is increased. With the use of conventional metrics, solar panel thermal image quality has been verified. The results obtained from ANNOVA also show the highest correlation coefficient. The same has been experimentally verified that the old panels give less power output compared to the new panels.

Data Availability

The data used to support the findings of this study are included within the article. Further data or information is available from the corresponding author upon request.

Conflicts of Interest

The authors declare that there are no conflicts of interest regarding the publication of this paper.

Acknowledgments

References

[1] A. Mellit, G. M. Tina, and S. A. Kalogirou, "Fault detection and diagnosis methods for photovoltaic systems: a review," *Renewable and Sustainable Energy Reviews*, vol. 91, pp. 1–17, 2018.

[2] P. Raju, K. Raja, K. Lingadurai, T. Maridurai, and S. C. Prasanna, "Glass/Caryota urens hybridized fibre-reinforced nanoclay/SiC toughened epoxy hybrid composite: mechanical, drop load impact, hydrophobicity and fatigue behaviour," *Biomass Conversion and Biorefinery*, vol. 2021, 2021.

[3] E. Kaplani, "Detection of degradation effects in field-aged c-Si solar cells through IR thermography and digital image processing," *International Journal of Photoenergy*, vol. 2012, 11 pages, 2012.

[4] V. Vignesh Kumar, K. Raja, V. S. Chandra Sekar, and T. Ramkumar, "Thrust force evaluation and microstructure characterization of hybrid composites (Al7075/B4C/BN) processed by conventional casting technique," *Journal of the Brazilian Society of Mechanical Sciences and Engineering*, vol. 41, no. 5, p. 228, 2019.

[5] E. M. Natsheh and A. Albarbar, "SSolar power plant performance evaluation: simulation and experimental validation," *Journal of Physics: Conference Series*, vol. 364, article 012122, 2012.

[6] V. Jeyabalaji, G. R. Kannan, P. Ganeshan, K. Raja, B. NagarajaGanesh, and P. Raju, "Extraction and characterization studies of cellulose derived from the roots ofAcalypha indicaL," *Journal of Natural Fibers, Taylor & Francis*, vol. 2021, pp. 1–13, 2021.

[7] M. H. Ali, A. Rabhi, A. El Hajjaji, and G. M. Tina, "Real time fault detection in photovoltaic systems," *Energy Procedia*, vol. 111, pp. 914–923, 2017.

[8] N. Akshaykumar and D. Subbulekshmi, "Online auto selection of tuning methods and auto tuning PI controller in FOPDT real time process-pH neutralization," *Energy Procedia*, vol. 117, pp. 1109–1116, 2017.

[9] A. M. Salazar and E. Q. B. Macabebe, "Hotspots detection in photovoltaic modules using infrared thermography," in *MATEC web of conferences*, vol. 70, pp. 1–5, Spain, August 2016.

[10] D. Subbulekshmi and J. Kanakaraj, "GMC algorithm with IMC and other controllers for a chemical process," *Journal of Advanced Engineering Technology*, vol. I, pp. 18–21, 2012.

[11] G. Radhaboy, M. Pugazhvadivu, P. Ganeshan, and K. Raja, "Influence of kinetic parameters on Calotropis procera by TGA under pyrolytic conditions," *Energy Sources Part A-Recovery Utilization and Environmental Effects*, vol. 2019, 2019.

[12] Y. Hu, W. Cao, J. Ma, S. J. Finney, and D. Li, "Identifying PV module mismatch faults by a thermography-based temperature distribution analysis," *IEEE Transactions on Device and Materials Reliability*, vol. 14, no. 4, pp. 951–960, 2014.

[13] F. A. Khan, B. K. Gautam, and S. Singh, "Detection of defects in solar panels using thermal imaging by PCA and ICA method," *International Research Journal of Engineering and Technology*, vol. 4, no. 6, pp. 1700–1703, 2017.

[14] K. Raja, V. S. Chandra Sekar, V. Vignesh Kumar, T. Ramkumar, and P. Ganeshan, "Microstructure characterization and performance evaluation on AA7075 metal matrix composites using RSM technique," *Arabian Journal for Science and EngineeringArabian Journal for Science and Engineering*, vol. 45, no. 11, pp. 9481–9495, 2020.

[15] S. Guesmi, K. Jamoussi, and M. Ghariani, "Efficiency improvement of PV module using an electrical thermal model," *Journal of Electrical Systems*, vol. 16, no. 2, pp. 246–256, 2020.

[16] V. Yamunadevi, G. Vijayanand, P. Ganeshan, S. Sowmiya, and K. Raja, "Effect on the behaviour of dynamic mechanical analysis for hybrid epoxy nanocomposite," *Materials Today: Proceedings*, vol. 37, pp. 223–227, 2021.

[17] D. M. D. Preethi and V. E. Jayanthi, "Performance analysis of iris-based identification system based on exudates," *International Journal of Biomedical Engineering and Technology*, vol. 29, no. 3, pp. 231–245, 2019.

[18] V. E. Jayanthi, V. Rajamani, and P. Karthikayen, "Performance analysis for geometrical attack on digital image watermarking," *International Journal of Electronics*, vol. 98, no. 11, pp. 1565–1580, 2011.

[19] N. Saravanan, V. Yamunadevi, V. Mohanavel et al., "Effects of the interfacial bonding behavior on the mechanical properties of E-glass fiber/nanographite reinforced hybrid composites," *Advances in Polymer Technology*, vol. 2021, 9 pages, 2021.

[20] Y. Yang, Q. Chen, and Y. Wan, "A fast near-optimum block truncation coding method using a truncated _K_ -means algorithm and inter-block correlation," *AEU-International Journal of Electronics and Communications*, vol. 65, no. 6, pp. 576–581, 2011.

[21] R. Ramkumar, R. Prabu, V. Yamunadevi, P. Saravanan, and P. Ganeshan, "Wear analysis of woven glass / nanofiller fiber reinforced hybrid composites," *Materials Today: Proceedings, Elsevier*, vol. 2020, 2020.

[22] A. Jaiswal, J. Upadhyay, and A. Somkuwar, "Image denoising and quality measurements by using filtering and wavelet based techniques," *AEU-International Journal of Electronics and Communications*, vol. 68, no. 8, pp. 699–705, 2014.

[23] P. Sainath, F. Mohammed Ajmal Sheriff, and P. Ganeshan, "Fabrication of hybrid polyester composites in various combinations and evaluate the mechanical properties," *Materials Today: Proceedings, Elsevier*, vol. 2020, 2020.

[24] M. Kutter and F. A. Petitcolas, "A fair benchmark for image watermarking systems," *Security and Watermarking of Multimedia Contents*, vol. 3657, pp. 25–27, 1999.